Peculiarities of Magnetoresistive Properties of $(Fe_{80}Co_{20})_xCu_{1-x}$ Film Alloy Prepared by Layer-by-Layer Condensation with Post-Annealing

I.M. Pazukha[a], D.I. Saltykov[b] and Y.O. Shkurdoda[a]

[a] *Sumy State University, Rymsky-Korsakov St. 2, 40007 Sumy, Ukraine*
[b] *Sumy State Pedagogical University named after A.S. Makarenko, Romens'ka St. 87, 40002 Sumy, Ukraine*

Received: 19.02.2022 & Accepted: 04.04.2022

Doi: 10.12693/APhysPolA.141.608 *e-mail: i.pazuha@aph.sumdu.edu.ua

The work is devoted to the results of investigations of magnetoresistive properties of $(Fe_{80}Co_{20})_xCu_{1-x}$ film alloy prepared by layer-by-layer condensation with post-annealing at the temperature of 550 K. The total thickness of the samples ranged from 20 to 50 nm. It has been demonstrated that the samples are homogeneous in thickness. At the concentration of Cu atoms of 50 at.%, as a result of spin-dependent electron scattering, the isotropic nature of magnetoresistance with the value of 0.5–1% is observed. It confirms the efficiency of the proposed method for the preparation of granular film with giant magnetoresistance. The annealing of film alloys at the temperature of 700 K does not change the nature of magnetoresistance. At the concentration of Cu atoms of less than 50 at.%, the anisotropic magnetoresistance is fixed only.

topics: film alloy, crystal structure, annealing, magnetoresistance

1. Introduction

Over the past decades, magnetic thin films have received considerable attention due to their scientific interests and practical application in different fields: electronics, magnetic sensors, nonlinear optics, electromagnetic shielding, etc. '[1–4]. As a result, magnetic materials like Fe and Co, and their binary and ternary alloys are widely investigated, with their magnetic, magnetoresistive, etc., properties experiencing rapid improvement [5–9]. For example, bulk Fe–Co alloys are well-known soft magnetic materials. However, their coercivity or saturation magnetization can be improved by their substitution into multilayer systems [10, 11] and heterogeneous granular systems [12, 13]. For example, Tekgül A. et al. [10] demonstrated that the magnetic (the coercivity and saturation magnetization) properties of the multilayers FeCo/Cu are significantly affected by magnetic layer thicknesses. Besides, results presented in [10] indicate that the thin non-magnetic layers with a thickness of 0.5 nm can provide the FeCo/Cu multilayers to show the giant magnetoresistance (GMR) effect of 5.5%. In the case of granular systems, the magnetic and magnetoresistive properties are closely related to the composition of the films and features of magnetic grains (size, shape, and distribution) [14, 15].

In this paper, we prepared the granular film alloy based on the $Fe_{80}Co_{20}/Cu/Fe_{80}Co_{20}$ three-layer system by post-annealing at 550 K. The purpose of our investigation is to study the efficiency of such method for preparation granular film with GMR.

2. Experimental detail

The film samples based on ferromagnetic alloy $Fe_{80}Co_{20}$ and Cu were evaporated on a glass–ceramic substrate using layer-by-layer electron-beam evaporation from two independent sources for $Fe_{80}Co_{20}$ and Cu in the vacuum chamber (the base pressure $p \sim 10^{-4}$ Pa). Namely, at the first stage of granular film alloy preparation, $Fe_{80}Co_{20}/Cu/Fe_{80}Co_{20}$ three-layer films were obtained. The thickness of the samples was controlled by two independent *in situ* quartz resonators with a precision of ±5 %. For the production of ternary alloy, the method of post-annealing at the temperature of 550 K was used. According to our previous investigations, the annealing process leads to the formation of a granular state [16]. As a result, a series of $(Fe_{80}Co_{20})_xCu_{1-x}/S$ film alloys with a total thickness within the range from 20 to 50 nm and a concentration of Cu atoms from 5 to 50 at.% was formed. The component concentration c_i was calculated based on the effective thickness of metal layers

$$c_i = \frac{d_i\,\rho_i\,\mu_i^{-1}}{d_1\,\rho_1\,\mu_1^{-1} + d_2'\,\rho_2\,\mu_2^{-1} + d_2''\,\rho_3\,\mu_3^{-1}}, \qquad (1)$$

where d_i is the thickness of the Cu layer, d_2' and d_2'' are an effective thickness of the layers that can be formed based on Co and Fe atoms, and ρ_i and μ_i are the density and molar mass of elements, respectively. The composition of the films was also determined using a scanning electron microscope (Tescan VEGA3) with an energy-scattering X-ray (EDX) detector (Oxford Instruments).

The crystal structure was studied using transmission electron microscopy in electronography mode (TEM-125K). A qualitative analysis of the elemental composition of the films was performed by secondary-ion mass spectrometry (SIMS) using a mass-spectrometer MS-7201M. The data obtained in layer-by-layer etching of the films with argon ions were used to plot the concentration profiles along with the sample depth.

The longitudinal and transverse magnetoresistance (the magnetic field in the film plane) measurements and thermomagnetic treatment of thin films were carried out in magnetic fields in the range of 200 mT in a special device in an ultrahigh oil-free vacuum (the base pressure of 10^{-6}–10^{-7} Pa). The value of magnetoresistance (MR) was calculated from

$$\mathrm{MR} = \frac{R(B)-R(B_c)}{R(B_c)}, \qquad (2)$$

where $R(B)$ is the resistance of the sample in the magnetic field with induction B, and $R(B_c)$ is the resistance of the sample in the magnetic field with a coercivity B_c.

3. Experimental results and discussion

The phases of $(Fe_{80}Co_{20})_xCu_{1-x}$/S film alloy by TEM, with the patterns, are shown in Fig. 1c. For more detailed analysis, the additional investigations of the $Fe_{80}Co_{20}$ film alloy phase state after annealing at 700 K (Fig. 1a) were done. For $Fe_{80}Co_{20}$ film alloy, all rings can be indexed to the body-centered cubic structure (bcc) FeCo with a lattice parameter a = 0.292–0.293 nm. The addition of Cu interlayer and formation of $(Fe_{80}Co_{20})_{60}Cu_{40}$ ternary alloy result in the eutectic state formation. The phase state corresponds to a combination of bcc-Fe_xCo_{1-x} and face-centered cubic solid solutions (fcc-ss) (Fig. 1(c)). The lattice of the solid solution (ss) has a tetragonal distortion, so it can be interpreted as the fcc lattice (for more details, see [16]).

Figure 1 shows bright-field TEM images of annealed at 700 K $Fe_{80}Co_{20}$/S (b) and $(Fe_{80}Co_{20})_{60}Cu_{40}$/S (d) film alloys. In Fig. 1b, the $Fe_{80}Co_{20}$/S film alloy consists of fine-dispersed grains with an average size of 20–30 nm. Note that substituting the Fe and Co atoms in the alloys results in no sharp grain faceting. The formation of $(Fe_{80}Co_{20})_{60}Cu_{40}$/S film alloys (Fig. 1d) leads to the formation of a granular structure in which ferromagnetic grains are embedded in a non-magnetic matrix of ss Cu(Fe, Co). In this case, the narrow parts of grains have sharp faceting with a stacking fault. According to [17], such growth origin is most likely for this type of sample. The grain size value ranges from 30 to 50 nm.

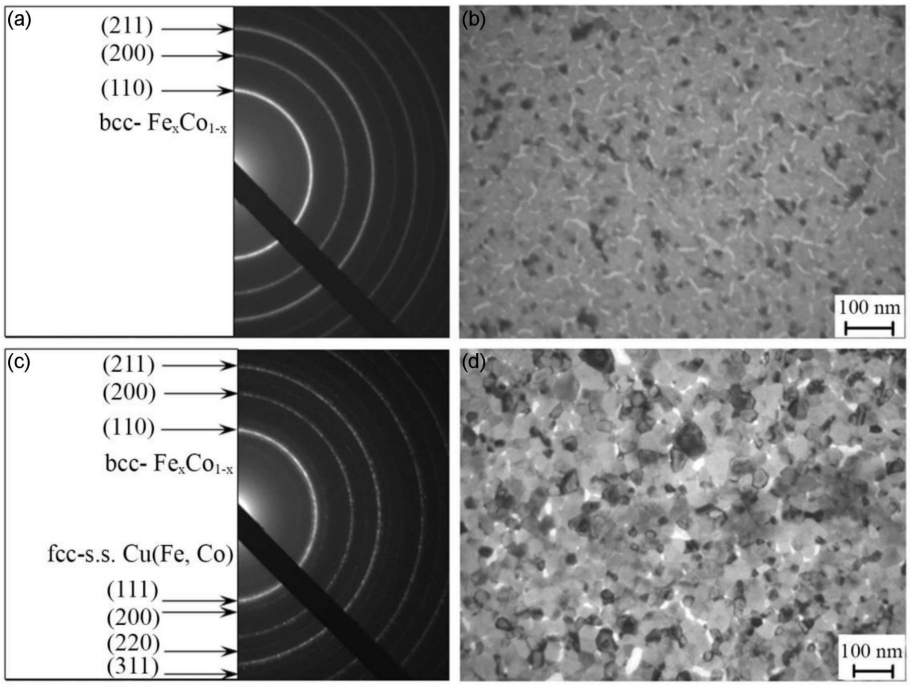

Fig. 1. Diffraction patterns and bright-field TEM images of annealed at 700 K $Fe_{80}Co_{20}$ (a, b) and $(Fe_{80}Co_{20})_{60}Cu_{40}$ (c, d) film alloys with a total thickness $d = 40$ nm.

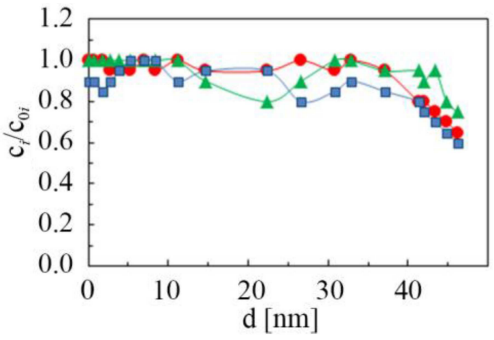

Fig. 2. The concentration profiles of the $(Fe_{80}Co_{20})_{50}Cu_{50}$/S films (◯ — Fe, △ — Cu, □ — Co) after annealing at 700 K. The concentration of the i-th element at the thickness change is c_i. The maximum concentration of the i-th element is c_{0i}, and d stands for thickness.

Figure 2 shows the results of research on the distribution of the concentration of the $(Fe_{80}Co_{20})_{50}Cu_{50}$/S film alloy components versus the thickness of the sample. It was made based on secondary ion mass spectrometry investigations. The concentration profiles indicate that the ternary alloys received by the method of layer-by-layer condensation with post-annealing up to 700 K are homogeneous in thickness. This result confirms the efficiency of the selected method of film alloy preparation.

The magnetoresistive properties of investigated samples are highly dependent on the sample's composition. Namely, the nature of the MR effect and its magnitude for samples with c_{Cu}=20 at.% were to be different from those of c_{Cu}=50 at.%. The magnetoresistive curve of $(Fe_{80}Co_{20})_{80}Cu_{20}$/S film alloy with thickness d = 40 nm is plotted in Fig. 3a. To make the measurements, the magnetic field was applied both parallel and perpendicular to the current flowing in the film plane to measure the longitudinal and transverse magnetoresistance, respectively. Note that measurements were done at room temperature. As seen in Fig. 3, the longitudinal MR value is positive, and transverse MR is negative. So, the nature of the field dependence of magnetoresistance is anisotropic. It can be seen that the shape of MR(B) curves is similar to the corresponding dependencies for pure ferromagnetic metals and ferromagnetic alloys [18, 19]. Hence, in the case of a low concentration of Cu atoms, the formation of an infinite ferromagnetic cluster occurs.

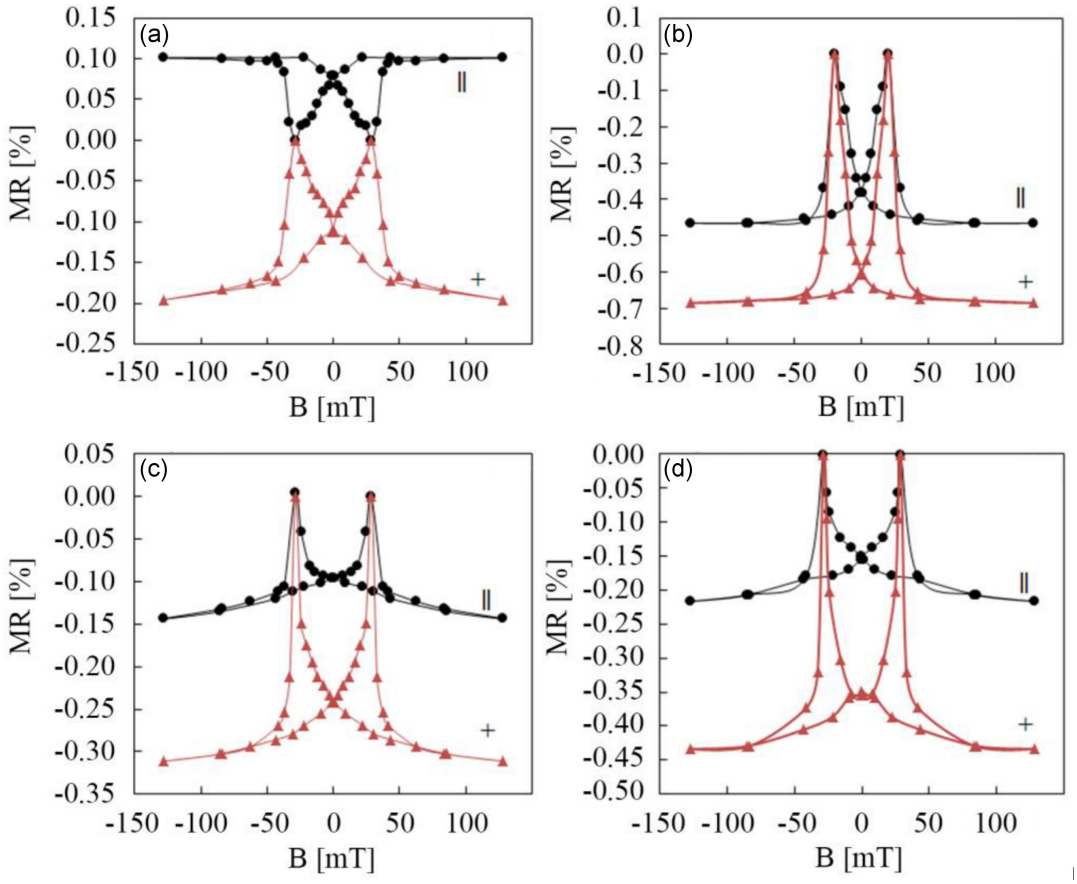

Fig. 3. The field dependence of longitudinal (||) and transverse (+) magnetoresistance for film alloy $(Fe_{80}Co_{20})_xCu_{1-x}$/S with d = 40 nm, and c_{Cu} = 20 at.% (a) and 50 at.% (b–d) after formation (a, b) and heat treatment at 700 K (c, d). The measurement temperatures are 300 K (a–c) and 120 K (d).

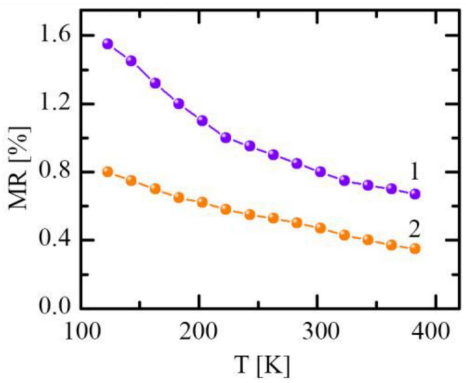

Fig. 4. Temperature dependence of isotropic magnetoresistance for $(Fe_{80}Co_{20})_xCu_{1-x}$/S film alloy ($c_{Cu} = 50$ at.%, $d = 40$ nm) after formation (line 1) and heat treatment at 700 K (line 2).

With an increase of the concentration of Cu atoms to 50 at.% (Fig. 3b), the longitudinal and transverse magnetoresistance decrease when the applied magnetic field increases, which means that the MR effect has an isotropic nature. The value of magnetoresistance of 0.5–1% was observed. The reason for the appearance of isotropic magnetoresistance is the granular state formation, as confirmed by electron microscopic investigations. As a result, the mechanism of spin-dependent electron scattering is realized.

The thermal stability of magnetic thin films is still an important research topic due to their wide practical application [20, 21]. Therefore, the investigations of the heat treatment effect in magnetoresistive properties of the film ternary alloy were done. For this purpose, the samples were annealed at 700 K for 20 min in a vacuum chamber, then cooled and investigated after annealing.

The annealing process at 700 K does not change the nature of field dependence of magnetoresistance, but their value decreases to 0.1–0.2 % (Fig. 3c). At the same time, more differences between the values of longitudinal and transverse magnetoresistance appear. The reason for such differences is the influence of the anisotropic magnetoresistance of the ferromagnetic component. The decrease in the measurement temperature to 120 K leads to an increase in the isotropic magnetoresistance value by 1.2–1.8 times (Fig. 3d).

The temperature dependence of isotropic magnetoresistance within the temperature range of 120–400 K was investigated. As an example, the MR(T) dependence for $(Fe_{80}Co_{20})_xCu_{1-x}$/S film alloy ($c_{Cu} = 50$ at.%, $d = 40$ nm) after formation and heat treatment at 700 K are presented in Fig. 4. As can be seen, the value of the isotropic magnetoresistance is decreased by 2–2.3 times with an increase in the temperature from 120 to 400 K. Note that the MR value decreases close to linear law with an increase in temperature.

There are two main contributions to the temperature dependence of GMR magnitude, i.e., inelastic phonon scattering and magnon scattering. The phonon scattering does not influence the electron spin. However, it is spin-dependent since the density of electronic states at the Fermi level is different for the majority and minority subbands. Phonon scattering reduces the electron mean free path, especially in a non-magnetic matrix. This reduces the flow of electrons between the ferromagnetic granules, which leads to a decrease in the value of the isotropic magnetoresistance. The contribution of magnon scattering at 300 K depends on how much the Curie temperature of the magnetic element differs from room temperature. Magnon scattering causes the spin-flip of conduction electrons, which leads to mixing between the two channels of the spin current.

4. Conclusions

In this work, $(Fe_{80}Co_{20})_xCu_{1-x}$/S film alloys were successfully prepared by the method of layer-by-layer condensation with post-annealing at 550 K. The main findings can be summarized as follows:

- The $(Fe_{80}Co_{20})_xCu_{1-x}$/S granular film alloy at $c_{Cu} = 5$–50 at.% after annealing up to 700 K has a phase state, which corresponds to the eutectic of the bcc Fe_xCo_{1-x} and fcc-ss Cu(Fe, Co).
- The secondary ion mass spectrometry results showed that received ternary alloys are homogeneous in thickness.
- Magnetoresistance measurements reveal that samples with $d = 20$–50 nm and $c_{Cu} = 50$ at.% are characterized by isotropic magnetoresistance, which values depend on their total thickness and the heat treatment temperature.
- It is confirmed that the decrease of the measurement temperature to 120 K allows to enhance the magnetoresistive effect 1.7–2 times.

Acknowledgments

This work was funded by the State Program of the Ministry of Education and Science of Ukraine 0120U102005.

References

[1] M. Carpentieri, G. Finocchio, *Encyclopedia of Smart Materials* **5**, 95 (2022).

[2] U.P. Borole, S. Subramaniam, I.R. Kulkarni, P. Saravanan, H.C. Barshilia, P. Chowdhury, *Sens. Actuat. A: Phys.* **280**, 125 (2018).

[3] V.V. Kondalkar, X. Li, I. Park, S.S. Yang, K. Lee, *Sci. Rep.* **8**, 2401 (2018).

[4] S. Mangin, M. Gottwald, C.-H. Lambert, D. Steil, V. Uhlíř, L. Pang, M. Hehn, S. Alebrand, M. Cinchetti, G. Malinowski, Y. Fainman, M. Aeschlimann, E.E. Fullerton, *Nat. Mater.* **13**, 286 (2014).

[5] S.P. Patel, T. Basu, M. Kumar, P. Mishra, T. Som, *Mater. Lett.* **308**, 131099 (2022).

[6] N.N. Li, M.X. Qiu, N. Wang, *J. Alloys Compd.* **747**, 250 (2018).

[7] R. Zhang, C. Zhou, K. Chen, K. Cao, Y. Zhang, F. Tian, A. Murtaza, S. Yang, X. Song, *Scr. Mater.* **203**, 114043 (2021).

[8] G. Durak Yüzüak, E. Yüzüak, I. Ennen, A. Hütten, *Curr. Appl. Phys.* **29**, 33 (2021).

[9] O. Adam, V. Jan, Z. Spotz, J. Cupera, V. Pouchly, *Mater. Charact.* **182**, 111532 (2021).

[10] A. Tekgül, M. Alper, H. Kockar, *J. Magn. Magn. Mater.* **421**, 472 (2017).

[11] I.L. Graff, A. Traverse, J. Geshev, S.R. Teixeira, L. Amaral, *Nucl. Instrum. Methods Phys. Res. B: Beam Interact. Mater. At.* **257**, 424 (2007).

[12] I. Kanada, A. Cruce, T. Mewes, S. Wu, C. Mewes, G. Mankey, T. Suzuki, *AIP Adv.* **7**, 056105 (2017).

[13] I.M. Pazukha, V.V. Shchotkin, Y.O. Shkurdoda, *Prog. Phys. Met.* **20**, 672 (2019).

[14] Ch. Wang, Y. Rong, T.Y. Hsu, *J. Magn. Magn Mater.* **305**, 310 (2006).

[15] Ch. Wang, Y. Zhang, X. Xiao, Y. Rong, H.Y. Tsu, *J. Mater. Sci.* **42**, 5903 (2007).

[16] D.I. Saltykov, Yu.O. Shkurdoda, I.Yu. Protsenko, *J. Nano- Electron. Phys.* **10**, 03024 (2018).

[17] D. Hull, D.J. Bacon, *Introduction to Dislocations*, 5th Ed., Butterworth-Heinemann, 2011.

[18] S.I. Vorobiov, Ia.M. Lytvynenko, I.O. Shpetnyi, O.V. Shutyleva, A.M. Chornous, *Metallofiz. Noveishie Tekhnol.* **37**, 1049 (2015).

[19] Kaushalya, S. Husain, V. Barwal, N.K. Gupta, S. Hait, S. Chaudhary, *Phys. B: Cond. Matter.* **570**, 1 (2019).

[20] Kh. Gheisari, C.K. Ong, *Phys. B* **595**, 412365 (2020).

[21] Yujin Li, Jiao Zhai, Lican Zhao, Jinping Chen, Xueni Shang, Cuimeng Song, Jinchao Chen, Shuang Liu, Fanbin Meng, *J. Solid State Chem.* **276**, 19 (2019).